GA

MP

IA

TURBULENT MULTIPHASE THERMAL FLOW MODELING OF DEFECT FORMATION MECHANISMS AND ELECTROMAGNETIC FORCE EFFECTS IN CONTINUOUS STEEL CASTING

Allocation: Illinois/75 Knh
PI: Brian G. Thomas[1]
Co-PIs: Seong–Mook Cho[2], Hyunjin Yang[1], Surya Pratap Vanka[1], Matthew Zappulla[2], Seid Koric[1,3], Ahmed Taha[3]

[1]University of Illinois at Urbana–Champaign
[2]Colorado School of Mines
[3]National Center for Supercomputing Applications

EXECUTIVE SUMMARY

Multiphysics models have been developed to quantify the formation mechanisms of various defects related to flow instability, particle transport and capture, superheat transport, surface depression, and cracking in continuous steel casting. To simulate these complex and interrelated phenomena more accurately, the research team implemented a commercial computational fluid dynamics program, ANSYS Fluent high-performance computing (HPC), and the multi-GPU-based in-house CUFLOW codes on Blue Waters' XE and XK nodes, respectively. Using these codes on Blue Waters' resources, various turbulent flow models including large-eddy simulations and Reynolds-averaged Navier–Stokes models have been coupled with the volume of fluid method, discrete phase model, particle capture models, and heat transfer models. Finally, the team is applying these models with magnetohydrodynamics (MHD) models to investigate the effects of electromagnetic systems (static or moving magnetic fields) on defect formation, such as longitudinal cracks and hooks, and to explore practical strategies for reducing defects in the process.

RESEARCH CHALLENGE

Continuous casting is the dominant process used to solidify over 96% of steel produced in the world [1]. Thus, even small improvements can have tremendous industrial impact. Many defects in final steel products originate in the mold region of the process owing to transient phenomena, which include turbulent multiphase flow, particle transport and capture, heat transfer, solidification, and thermal–mechanical behavior. To reduce defect formation, various electromagnetic (EM) systems are often employed to control the transient turbulent flow and accompanying phenomena, according to the varying process conditions in the production facility [2]. Experiments and measurements to quantify these phenomena are extremely limited owing to the harsh environment and huge size of the process as well as the many process parameters. Therefore, the development of high-resolution computational models is an important tool to more accurately simulate and understand the process phenomena and defect formation and to find more practical ways to reduce defects and improve the process. Thus, the research team conducted multiphysics simulations on the Blue Waters supercomputer in order to quantify turbulent multiphase flow, argon gas bubble interaction and size distribution, particle transport and capture, and superheat transport, and to simulate the effects of moving magnetic fields on these phenomena, in order to investigate ways to reduce defects.

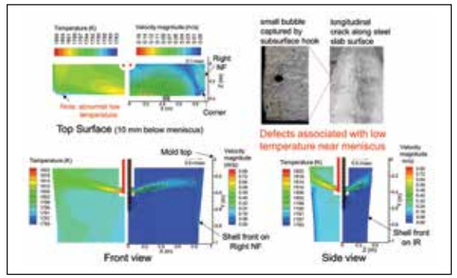

Figure 1: Mold flow pattern and resulting temperature distribution affect defect formation in continuous steel casting.

METHODS & CODES

The research team conducted large-eddy simulations (LES) coupled with the volume of fluid method to calculate transient behavior of three-dimensional surface slag/molten steel interface during continuous steel-slab casting [3]. The team used the hybrid multiphase turbulent flow model [4,5] that couples the Eulerian–Eulerian (EE) two-fluid model together with a discrete phase model (DPM) that was validated with lab-scale low-melting alloy experiments to simulate argon bubble interaction (gas pocket formation, gas expansion, breakup, and coalescence) and size distributions in a real slide-gate nozzle [6]. These models have been developed using a commercial computational fluid dynamics program, ANSYS Fluent HPC, on Blue Waters' XE nodes (AMD 6276 "Interlagos" processor). In addition, transport and capture of the argon bubbles were calculated using LES coupled with the DPM and advanced capture models [7], which were implemented on Blue Waters' XK nodes (NVIDIA GK110 "Kepler" accelerator) with the multi-GPU-based in-house code CUFLOW [8].

The team applied the magnetic-induction MHD model [2] together with the turbulent-flow models (LES/Reynolds-averaged Navier–Stokes models), the DPM of the transport and capture of inclusions and bubbles, and a heat transfer model, to investigate effects of moving magnetic fields, including EM level stabilizer, EM level accelerator, and mold EM stirring (M–EMS) [2] on the flow pattern and instability, gas bubble distribution, temperature distribution, and superheat at the shell solidification front in the slab mold during steady continuous casting.

RESULTS & IMPACT

Turbulent fluid flow, surface slag/molten steel interface instability, liquid-level fluctuations at the meniscus, slag entrainment, and entrapment were computed from the multiphysics model simulations. This allows understanding of slag defect formation mechanisms, especially the slag entrapment owing to sudden level drops near meniscus regions. From the validated EEDPM model [4,5] simulations, argon bubble behavior and size distributions in the turbulent molten-steel flow inside a slide-gate nozzle of the real caster [6] were revealed in detail. This calculation is expected to contribute to more accurate particle-capture results by being coupled with the advanced particle capture model [7].

In addition, the study investigated initial solidification-related defects such as meniscus freezing, hook formation [9,10], and longitudinal crack formation near the meniscus with the further aid of the coupled heat-transfer model. For example, in mega-thick slab casting, as shown in Fig. 1, the distribution of superheat flux around the mold perimeter was very nonuniform with the unoptimized mold flow pattern. In particular, superheat was unable to reach the meniscus corner, leading to deep hooks and/or longitudinal crack formation. In addition, the effect of the M–EMS on mold flow pattern, temperature, and superheat distribution was quantified from the magnetic-induction MHD model simulations. With M–EMS, the superheat flux at the shell front became more uniform owing to the rotating flow around the perimeter of the mold, resulting in higher superheat flux to the corners, as shown in Fig. 2. This effect is expected to lessen initial solidification defects, so long as the magnetic field strength is within an optimal range.

WHY BLUE WATERS

The high-resolution models used to more accurately simulate and better understand defect formation mechanisms in continuous steel casting are very computationally intensive. The many coupled governing equations need to be solved for turbulent flow, particle transport and capture, temperature, and MHD fields. Moreover, many computational cells are required to capture these complex and interrelated phenomena on micrometer and millisecond scale in the huge domain. Blue Waters enables such high-resolution simulations in a reasonable time frame by speeding up ANSYS Fluent HPC calculations by more than 3,000 times and CUFLOW calculations by 50 times. Furthermore, the Blue Waters parallel computing environment enables numerous cases to be calculated simultaneously with different process conditions for parametric studies essential to optimize this complex process. Thus, the Blue Waters supercomputer provides a great contribution to obtaining deep insights into complicated defect-related phenomena with high resolution in order to improve this important commercial process.

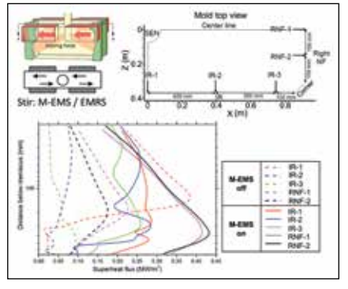

Figure 2: Effect of electromagnetic stirring on superheat flux profiles near the solidifying steel shell front around the perimeter of the mold.

PUBLICATIONS & DATA SETS

M. L. S. Zappulla, S. Koric, S.–M. Cho, H.–J. Lee, S.–H. Kim, and B. G. Thomas, "Multiphysics modeling of continuous casting of stainless steel," *J. Mater. Proc. Tech.*, vol. 278, p. 116469, 2020. doi: 10.1016/j.jmatprotec.2019.116469.

S.-M. Cho, M. Liang, H. Olia, L. Das, B. G. Thomas, "Multiphase flow-related defects in continuous casting of steel slabs" in *TMS 2020 149th Annual Meeting and Exhibition Supplemental Proceedings*, San Diego, CA, U.S.A., Feb. 23-27, 2020, pp 1161-1173. doi: 10.1007/978-3-030-36296-6.

S.–M. Cho, B. G. Thomas, and S.–H. Kim, "Effect of nozzle port angle on transient flow and surface slag behavior during continuous steel-slab casting," *Metall. Mater. Trans. B*, vol. 50B, no. 1, pp. 52–76, 2019, doi: 10.1007/s11663-018-1439-9.

S.–M. Cho and B. G. Thomas, "Modeling of transient behavior of top-surface slag/molten steel interface in continuous slab casting," presented at *STEELSIM 2019*, Toronto, Ont., Can., 2019.

M. L. S. Zappulla, S.–M. Cho, and B. G. Thomas, "Visualization of steel continuous casting including a new integral method for post-processing temperature data," *Steel Res. Int.*, vol. 90, pp. 1–11, 2019. doi: 10.1002/srin.201800540.

M. L. S. Zappulla and B. G. Thomas, "Surface defect formation in steel continuous casting," *Maters. Sci. Forum*, vol. 941, pp. 112–117, 2018, doi: 10.4028/www.scientific.net/MSF.941.112.

K. Jin, S. P. Vanka, and B. G. Thomas, "Large eddy simulations of electromagnetic braking effects on argon bubble transport and capture in a steel continuous casting mold," *Metall. Mater. Trans. B*, vol. 49B, no. 3, pp. 1360–1377, 2018, doi: 10.1007/s11663-018-1191-1.

H. Yang, S. P. Vanka, and B. G. Thomas, "A hybrid Eulerian–Eulerian discrete-phase model of turbulent bubbly flow," *J. Fluids Eng.*, vol. 140, no. 10, p. 101202, 2018, doi: 10.1115/1.4039793.

H. Yang, S. P. Vanka, and B. G. Thomas, "Modeling of argon gas behavior in continuous casting of steel," *JOM*, vol. 70, no. 10, pp. 2148–2156, 2018, doi: 10.1007/s11837-018-2997-7.

H. Yang, S. P. Vanka, and B. G. Thomas, "Modeling of argon gas behavior in continuous casting of steel," in *CFD Modeling and Simulation in Materials Processing 2018*, Warrendale, PA, U.S.A.: Springer, 2018, pp. 119–131. doi: 10.1007/978-3-319-72059-3_9

S.–M. Cho and B. G. Thomas, "1) LES modeling of slag entrainment and entrapment and 2) Nozzle flow model validation with measurements of pressure-drop and bubble-size distribution," *CCC Annual Report*, 2018.

L. Matthew, S. Zappulla, and B. G. Thomas, "Modeling and online monitoring with fiber-Bragg sensors of surface defect formation during solidification in the mold," *CCC Annual Report*, 2018.

[3] L. Jay, H. Kim, Y. Saad, and J. Chelikowsky, "Electronic structure calculations for plane-wave codes without diagonalization," *Comput. Phys. Comm.*, vol. 118, no. 1, pp. 21–30, 1999.
[4] A. Niklasson, C. Tymczak, and M. Challacombe, "Trace resetting density matrix purification in O(N) self-consistent-field theory," *J. Chem. Phys.*, vol. 118, no. 19, pp. 8611–8620, 2003.
[5] H. H. Rosenbrock, "Some general implicit processes for the numerical solution of differential equations," *Comput. J.*, vol. 5, no. 4, pp. 329–330, 1963.
[6] C. Moler and C. Van Loan, "Nineteen dubious ways to compute the exponential of a matrix," *SIAM Rev.*, vol. 20, no. 4, pp. 801–836, 1978.
[7] C. Moler and C. Van Loan, "Nineteen dubious ways to compute the exponential of a matrix, twenty-five years later," *SIAM Rev.*, vol. 45, no. 2, pp. 3–49, 2003.
[8] V. V. Dobrovitski and H. A. De Raedt, "Efficient scheme for numerical simulations of the spin-bath decoherence," *Phys. Rev. E*, vol. 67, no. 5, p. 056702, 2003.
[9] B. A. Shadwick and W. F. Buell, "Unitary integration: A numerical technique preserving the structure of the quantum Liouville equation," *Phys. Rev. Lett.*, vol. 79, no. 26, p. 5189, 1997.

Koric, Seid

[1] S. Koric and A. Gupta, "Sparse matrix factorization in the implicit finite element method on petascale architecture," *Comput. Methods in Appl. Mech. Eng.*, vol. 302, p. 281, Apr. 2016.
[2] C. Ashcraft *et al.*, "Increasing the scale of LS–DYNA implicit analysis," presented at 15th Inter. LS–DYNA Conf., Detroit, MI, USA, Jun. 2018.
[3] C. Ashcraft *et al.*, "Running jet engine models on thousands of processors with LS–DYNA implicit," presented at the 12th European LS–DYNA Conf., Koblenz, Germany, May 2019.
[4] T. A. Simons *et al.*, "Reducing the time-to-solution for finite element analysis of gas turbine engines," presented at the AIAA Propulsion and Energy Forum and Exposition, Indianapolis, IN, USA, Aug. 2019.

Leburton, Jean–Pierre

[1] A. Tubbs and A. Nussenzweig, "Endogenous DNA damage as a source of genomic instability in cancer," *Cell*, vol. 168, no. 4, pp. 644–656, 2017.
[2] W. Humphrey, A. Dalke, and K. Schulten, "VMD: Visual molecular dynamics," *J. Mol. Graphics*, vol. 14, no. 1, pp. 33–38, 1996.
[3] N. Foloppe and J. A. D. Mackerell, "All-atom empirical force field for nucleic acids: I. Parameter optimization based on small molecule and condensed phase macromolecular target data," *J. Comput. Chem.*, vol. 21, no. 2, pp. 86–104, 2000.
[4] A. Aksimentiev, J. B. Heng, G. Timp, and K. Schulten, "Microscopic kinetics of DNA translocation through synthetic nanopores," *Biophys. J.*, vol. 87, no. 3, pp. 2086–2097, 2004.
[5] A. Girdhar, C. Sathe, K. Schulten, and J.–P. Leburton, "Graphene quantum point contact transistor for DNA sensing," *Proc. Nat. Acad. Sci. USA*, vol. 110, no. 42, pp. 16748–16753, 2013.
[6] A. Sarathy and J.–P. Leburton, "Electronic conductance model in constricted MoS_2 with nanopores," *Appl. Phys. Lett.*, vol. 108, no. 5, p. 053701, 2016.
[7] N. B. M. Athreya, A. Sarathy, and J.–P. Leburton, "Large scale parallel DNA detection by two-dimensional solid-state multipore systems," *ACS Sensors*, vol. 3, no. 5, pp. 1032–1039, 2018.

Mashayek, Farzad

[1] D. A. Kopriva and J. H. Kolias, "A conservative staggered-grid Chebyshev multidomain method for compressible flows," *J. Comput. Phys.*, vol. 125, no. 1, pp. 244–261, Apr. 1996.
[2] D. A. Kopriva, "A staggered-grid multidomain spectral method for the compressible Navier–Stokes equations," *J. Comput. Phys.*, vol. 143, no. 1, pp. 125–158, Jun. 1998.
[3] G. B. Jacobs, D. A. Kopriva, and F. Mashayek, "Validation study of a multidomain spectral code for simulation of turbulent flows," *AIAA J.*, vol. 43, no. 6, pp. 1256–1264, May 2005.

Matalon, Moshe

[1] M. Matalon and B. J. Matkowsky, "Flames as gasdynamic discontinuities, *J. Fluid Mech.*, vol. 124, pp. 239–259, 1982.
[2] M. Matalon, C. Cui, and J. K. Bechtold, "Hydrodynamic theory of premixed flames: Effects of stoichiometry, variable transport coefficients and arbitrary reaction orders," *J. Fluid Mech.*, vol. 487, pp.179–210, 2003.
[3] A. Patyal and M. Matalon, "Nonlinear development of hydrodynamically-unstable flames in three-dimensional laminar flows," *Combust. Flame*, vol. 195, pp. 128–139, 2018.

Raman, Venkat

[1] K. Y. Cho, J. R. Codoni, B. A. Rankin, J. Hoke, and F. Schauer, "High-repetition-rate chemiluminescence imaging of a rotating detonation engine," presented at the 54th AIAA Aerospace Sciences Meeting, San Diego, CA, USA, Jan. 4–8, 2016, AIAA Paper 2016–1648.
[2] P. A. Cocks, A. T. Holley, and B. A. Rankin, "High fidelity simulations of a non-premixed rotating detonation engine," presented at the 54th AIAA Aerospace Sciences Meeting, San Diego, CA, USA, Jan. 4–8, 2016, AIAA Paper 2016–0125.
[3] B. A. Rankin *et al.*, "Chemiluminescence imaging of an optically accessible non-premixed rotating detonation engine," *Combust. Flame*, vol. 176, pp. 12–22, 2017.

Riedl, Caroline

[1] The DOE/NSF Nuclear Science Advisory Committee Working Group, *The Frontiers of Nuclear Science: A Long-Range Plan*, Dec. 2007, arXiv:0809.3137.
[2] COMPASS Collaboration, "First measurement of transverse-spin-dependent azimuthal asymmetries in the Drell–Yan process," *Phys. Rev. Lett.*, vol. 119, p. 112002, 2017.
[3] H. Riahi *et al.*, "FTS3: Quantitative monitoring," *J. Phys.*, Conference Series 664, p. 062051, 2015.
[4] J. Allison *et al.*, "Facilities and methods: Geant4—A simulation toolkit," *Nucl. Instrum. Methods Phys. Res. A*, vol. 506, pp. 250–303, 2003.
[5] The XXVII International Workshop on Deep Inelastic Scattering and Related Topics (DIS 2019), Apr. 8–12, 2019, Torino, Italy.

Schleife, André (1)

[1] M. Xu, T. Liang, M. Shi, and H. Chen, "Graphene-like two-dimensional materials," *Chem. Rev.*, vol. 113, no. 5, pp. 3766–3798, May 2013, doi: 10.1021/cr300263a.
[2] U. Bangert *et al.*, "Ion implantation of graphene—Toward IC compatible technologies," *Nano Lett.*, vol. 13, no. 10, Oct. 2013, doi: 10.1021/nl402812y.
[3] L. Vicarelli, S. Heerema, C. Dekker, and H. Zandbergen, "Controlling defects in graphene for optimizing the electrical properties of graphene nanodevices," *ACS Nano*, vol. 9, no. 4, Apr. 2015, doi: 10.1021/acsnano.5b01762.
[4] A. Schleife, E. Draeger, Y. Kanai, and A. Correa, "Plane-wave pseudopotential implementation of explicit integrators for time-dependent Kohn–Sham equations in large-scale simulations," *J. Chem. Phys.*, vol. 137, no. 22, Oct. 2012, doi: 10.1063/1.4758792.
[5] C. Ullrich, *Time-Dependent Density-Functional Theory: Concepts and Applications*. Oxford, UK, Oxford Univ. Press, 2013. [Online]. Available: doi: 10.1093/acprof:oso/9780199563029.001.0001
[6] S. Abhyankar, J. Brown, E. Constantinescu, D. Ghosh, B. Smith, and H. Zhang, "PETSc/TS: A modern scalable ODE/DAE solver library," Jun. 2018, arXiv:1806.01437 [math.NA].
[7] S. Balay, W. Gropp, L. McInnes, and B. Smith, "PETSc Users Manual," Tech. Rep. ANL–95/11—Revision 3.10, Argonne National Laboratory, 2018.

Schleife, André (2)

[1] S. A. Maier *et al.*, "Local detection of electromagnetic energy transport below the diffraction limit in metal nanoparticle plasmon waveguides," *Nature*, vol. 2, no. 4, p. 220, 2003.
[2] D. P. Fromm, A. Sundaramurthy, P. J. Schuck, G. Kino, and W. E. Moerner, "Gap-dependent optical coupling of single 'bowtie' nanoantennas resonant in the visible," *Nano Lett.*, vol. 4, no. 5, pp. 957–961, 2004.
[3] S. Prayakarao *et al.*, "Tunable VO_2/Au hyperbolic metamaterial," *App. Phys. Lett.*, vol. 109, no. 6, p. 061105, 2016.
[4] S. Kawata, A. Ono, and P. Verma, "Subwavelength colour imaging with a metallic nanolens," *Nat. Photonics*, vol. 2, no. 7, p. 438, 2008.
[5] N. Engheta, A. Salandrino, and A. Alu, "Circuit elements at optical frequencies: Nanoinductors, nanocapacitors, and nanoresistors," *Phys. Rev. Lett.*, vol. 95, no. 9, p. 095504, 2005.
[6] T. Stakenborg and L. Lagae, "Gold nanoring as a sensitive plasmonic biosensor for on-chip DNA detection," *App. Phys. Lett.*, vol. 100, no. 17, p. 173114, 2012.
[7] J. B. Khurgin and A. Boltasseva, "Reflecting upon the losses in plasmonics and metamaterials," *MRS Bull.*, vol. 37, no. 8, p. 768779, 2012.
[8] G. Kresse and J. Furthmüller, "Efficient iterative schemes for *ab initio* total-energy calculations using a plane-wave basis set," *Phys. Rev. B*, vol. 54, no. 16, pp. 11169–11186, 1996.
[9] A. Jain *et al.*, "The Materials Project: A materials genome approach to accelerating materials innovation," *APL Mat.*, vol. 1, no. 1, p. 011002, 2013.
[10] S. P. Ong *et al.*, "Python Materials Genomics (pymatgen): A robust, open-source python library for materials analysis," *Comp. Mat. Sci.*, vol. 68, pp. 314–319, Feb. 2013.
[11] F. Pedregosa *et al.*, "Scikit-learn: Machine learning in Python," *J. Mach. Learn. Res.*, vol. 12, pp. 2825–2830, 2011.

Thomas, Brian G.

[1] World Steel Association, "Table 4: Production of continuously cast steel," in *Steel Statistical Yearbook 2018*. Brussels, Belgium: World Steel Assoc., 2018, pp. 9–12.
[2] S.–M. Cho and B. G. Thomas, "Electromagnetic forces in continuous casting of steel slabs," *Metals (Spec. Issue: Cont. Casting)*, vol. 9, no. 4, pp. 1–38, 2019, doi: 10.3390/met9040471.
[3] S.–M. Cho, B. G. Thomas, and S.–H. Kim, "Effect of nozzle port angle on transient flow and surface slag behavior during continuous steel-slab casting," *Metall. Mater. Trans. B*, vol. 50B, no. 1, pp. 52–76, 2019, doi: 10.1007/s11663-018-1439-9.
[4] H. Yang, S. P. Vanka, and B. G. Thomas, "A hybrid Eulerian–Eulerian discrete-phase model of turbulent bubbly flow," *J. Fluids Eng.*, vol. 140, no. 10, p. 101202, 2018, doi: 10.1115/1.4039793.
[5] H. Yang, S. P. Vanka, and B. G. Thomas, "Modeling of argon gas behavior in continuous casting of steel," in *CFD Modeling and Simulation in Materials Processing 2018*, Warrendale, PA, USA: Springer, 2018, pp. 119–131.
[6] H. Yang, S. P. Vanka, and B. G. Thomas, "Modeling of argon gas behavior in continuous casting of steel," *JOM*, vol. 70, no. 10, pp. 2148–2156, 2018, doi: 10.1007/s11837-018-2997-7.

[7] K. Jin, S. P. Vanka, and B. G. Thomas, "Large eddy simulations of electromagnetic braking effects on argon bubble transport and capture in a steel continuous casting mold," *Metall. Mater. Trans. B*, vol. 49B, no. 3, pp. 1360–1377, 2018, doi: 10.1007/s11663-018-1191-1.
[8] S. P. Vanka, A. F. Shinn, and K. C. Sahu, "Computational fluid dynamics using graphics processing units: Challenges and opportunities," in *Proc. ASME 2011 IMECE Conf.*, pp. 429–437.
[9] J. Sengupta, B. G. Thomas, H. Shin, G. Lee, and S. Kim, "Mechanism of hook formation during continuous casting of ultra-low carbon steel slabs," *Metall. Mater. Trans. A*, vol. 37A, pp. 1597–1611, 2006.
[10] H. Shin, S. Kim, B. G. Thomas, G. Lee, J. Park, and J. Sengupta, "Measurement and prediction of lubrication, powder consumption, and oscillation mark profiles in ultra-low carbon steel slabs," *ISIJ Int.*, vol. 46, pp. 1635–1644, 2006.

Tinoco Lopez, Rafael O.

[1] E. W. Koch, "Beyond light: Physical, geological, and geochemical parameters as possible submersed aquatic vegetation habitat requirements," *Estuaries*, vol. 24, no. 1, pp. 1–17, 2001.
[2] H. M. Nepf, "Hydrodynamics of vegetated channels," *J. Hydraul. Res.*, vol. 50, no. 3, pp. 262–79, 2012.
[3] H. M. Nepf, "Flow and transport in regions with aquatic vegetation," *Ann. Rev. Fluid Mech.*, vol. 44, pp. 123–142. 2012.
[4] R. Tinoco and G. Coco, "A laboratory study on sediment resuspension within arrays of rigid cylinders," *Adv. Water Res.*, vol. 92, pp. 1–9, 2016.
[5] P. F. Fischer, J. W. Lottes, and S. G. Kerkemeier, *NEK5000 webpage*. (2008). [Online]. Available: https://nek5000.mcs.anl.gov
[6] M. Deville, P. F. Fischer, and E. Mund, *High-Order Methods for Incompressible Fluid Flow*. Cambridge, England: Cambridge Univ. Press, 2002.
[7] S. Dutta, M. I. Cantero, and M. H. Garcia, "Effect of self-stratification on sediment diffusivity in channel flows and boundary layers: A study using direct numerical simulations," *Earth Surf. Dyn.*, vol. 2, no. 2, p. 419, 2014.

Toussaint, Kimani

[1] Y. Hernandez *et al.*, "High-yield production of graphene by liquid-phase exfoliation of graphite," *Nat. Nanotechnol.*, vol. 3, no. 9, p. 563, 2008.
[2] M. Lotya *et al.*, "Liquid phase production of graphene by exfoliation of graphite in surfactant/water solutions," *J. Am. Chem. Soc.*, vol. 131, no. 10, pp. 3611–3620, 2009.
[3] V. Sresht, A. A. H. Pádua, and D. Blankschtein, "Liquid-phase exfoliation of phosphorene: Design rules from molecular dynamics simulations," *ACS Nano.*, vol. 9, no. 8, pp. 8255–8268, 2015.

Trinkle, Dallas R.

[1] S. L. Frederiksen, K. W. Jacobsen, K. S. Brown, and J. P. Sethna, "Bayesian ensemble approach to error estimation of interatomic potentials," *Phys. Rev. Lett.*, vol. 93, p. 165501, 2004.
[2] P. Zhang and D. R. Trinkle, "Database optimization for empirical interatomic potential models," *Model. Simul. Mater. Sci. Eng.*, vol. 23, p. 065011, 2015, doi: 10.1088/0965-0393/23/6/065011.
[3] P. Zhang and D. R. Trinkle, "A modified embedded atom method potential for interstitial oxygen in titanium," *Comp. Mater. Sci.*, vol. 124, pp. 204–210, 2016, doi: 10.1016/j.commatsci.2016.07.039.

Wagner, Lucas K.

[1] L. K. Wagner, M. Bajdich, and L. Mitas, "QWalk: A quantum Monte Carlo program for electronic structure," *J. Comput. Phys.*, vol. 228, pp. 3390–3404, 2009.

Wang, Zhi Jian

[1] S. Y. Han, R. Taghavi, and S. Farokhi, "Passive control of supersonic rectangular jets through boundary layer swirl," *Int. J. Turbo Jet-Eng.*, vol. 30, no. 2, pp. 199–216, Jun. 2013.
[2] Z. J. Wang *et al.*, "Towards industrial large eddy simulation using the FR/CPR method," *Comput. Fluids*, vol. 156, pp. 579–589, Oct. 2017.
[3] M. J. Lighthill, "On sound generated aerodynamically. I. General theory," *Proc. R. Soc. Lond. A*, vol. 222, pp. 564–587, 1952.
[4] H. T. Huynh, "A flux reconstruction approach to high-order schemes including discontinuous Galerkin methods," presented at the 18th AIAA Comput. Fluid Dyn. Conf., Miami, Florida, USA, Jun. 25–28, 2007.
[5] Z. J. Wang and H. Gao, "A unifying lifting collocation penalty formulation including the discontinuous Galerkin, spectral volume/difference methods for conservation laws on mixed grids," *J. Comput. Phys.*, vol. 228, pp. 8161–8186, 2009.
[6] C. K .W. Tam, "Supersonic jet noise," *Ann. Rev. Fluid Mech.*, vol. 27, pp. 17–43, 1995.

Wentzcovitch, Renata M.

[1] D. B. Zhang, T. Sun, and R. M. Wentzcovitch, "Phonon quasiparticles and anharmonic free energy in complex systems," *Phys. Rev. Lett.*, vol. 112, 2014, doi: 10.1103/PhysRevLett.112.058501.
[2] K. Sarkar, M. Topsakal, N. A. W. Holzwarth, and R. M. Wentzcovitch, "Evolutionary optimization of PAW data-sets for accurate high pressure simulations," *J. Computat. Phys.*, vol. 347, pp. 39–55, 2017, doi:10.1016/j.jcp.2017.06.032.

Xu, Bin

[1] H. F. Jansen and A. J. Freeman, "Total-energy full-potential linearized augmented-plane-wave method for bulk solids: Electronic and structural properties of tungsten," *Phys. Rev. B*, vol. 30, p. 561, 1984.
[2] M. Weinert, E. Wimmer, and A. J. Freeman, "Total-energy all-electron density functional method for bulk solids and surfaces," *Phys. Rev. B*, vol. 26, pp. 4571, 1982.

Xu, Zhen

[1] C. E. Brennen, *Cavitation and Bubble Dynamics*, Cambridge Univ. Press, 2013.
[2] T. Deplancke, O. Lame, J. Y. Cavaille, M. Fivel, M. Riondet, and J. P. Franc, "Outstanding cavitation erosion resistance of Ultra High Molecular Weight Polyethylene (UHMWPE) coatings," *Wear*, vol. 328–329, pp. 301–308, 2015.
[3] J. P. Franc, M. Riondet, A. Karimi, and G. L. Chahine, "Material and velocity effects on cavitation erosion pitting," *Wear*, vol. 274–275, pp. 248–259, 2012.
[4] *Advanced Experimental and Numerical Techniques for Cavitation Erosion Prediction*, K.–H. Kim, G. Chahine, J.–P. Franc, and A. Karimi, Eds., Springer, 2014.
[5] S. A. Beig and E. Johnsen, "Maintaining interface equilibrium conditions in compressible multiphase flows using interface capturing," *J. Comput. Phys.*, vol. 302, pp. 548–566, 2015.
[6] S. A. Beig, B. Aboulhasanzadeh, and E. Johnsen, "Temperatures produced by inertially collapsing bubbles near rigid surfaces," *J. Fluid Mech.*, vol. 852, pp. 105–125, 2018.
[7] M. Rodriguez and E. Johnsen, "A high-order, finite-difference approach for numerical simulations of shocks interacting with interfaces separating different linear viscoelastic materials," *J. Comput. Phys.*, vol. 379, pp. 70–90, 2019.
[8] M. Rodriguez, K. G. Powell, and E. Johnsen, "A high-order accurate AUSM+-up approach for simulations of compressible multiphase flows with linear viscoelasticity," *Shock Waves*, vol. 29, no. 5, pp. 717–734, 2019.

Yan, Yonghua

[1] C. Lee and R. Li, "Dominant structure for turbulent production in a transitional boundary layer," *J. Turbul.*, vol. 8, no. 55, p. N55, Jan. 2007.
[2] F. F. Grinstein, L. G. Margolin, and W. J. Rider, *Implicit Large Eddy Simulation*. Cambridge, UK: Cambridge Univ. Press, 2011.
[3] S. P. Spekreijse, "Elliptic grid generation based on Laplace equations and algebraic transformations," *J. Comput. Phys.*, vol. 118, no. 1, pp. 38–61, 1995.
[4] Y. Yan, L. Chen, Q. Li, and C. Liu, "Numerical study on microramp vortex generation for supersonic ramp flow control at Mach 2.5," *Shock Waves*, vol. 27, no. 1, pp 79–96, 2016.
[5] Y. Yan, C. Chen, P. Lu, and C. Liu, "Study on shock wave–vortex ring interaction by the micro vortex generator controlled ramp flow with turbulent inflow," *Aerosp. Sci. Technol.*, vol. 30, no. 1, pp. 226–231, 2013.
[6] Y. Yan, C. Chen, H. Fu, and C. Liu, "DNS study on Λ-vortex and vortex ring formation in flow transition at Mach number 0.5," *J. Turbul.*, vol. 15, no. 1, pp. 1–21, Jan. 2014.
[7] L. Jiang, H. Shan, C. Liu, and M. R. Visbal, "Non-reflecting boundary conditions for DNS in curvilinear coordinates," in *Recent Advances in DNS and LES: Proc. of the 2nd AFOSR Conf.*, New Brunswick, NJ, USA, Jun. 7–9, 1999, pp. 219–233.

Yeung, Pui–Kuen

[1] U. Frisch, *Turbulence. The Legacy of A.N. Kolmogorov*. Cambridge, UK: Cambridge Univ. Press, 1995.
[2] P. K. Yeung, K. R. Sreenivasan, and S. B. Pope, "Effects of finite spatial and temporal resolution on extreme events in direct numerical simulations of incompressible isotropic turbulence," *Phys. Rev. Fluids*, vol. 3, p. 064603, 2018.
[3] V. Yakhot and K. R. Sreenivasan, "Anomalous scaling of structure functions and dynamic constraints on turbulence simulations," *J. Stat. Phys.*, vol. 121, pp. 823–841, 2005.
[4] A. A. Migdal, "Loop equation and area law in turbulence," *Int. J. Mod. Phys. A*, vol. 9, pp. 1197–1238, 1994.
[5] K. R. Sreenivasan, A. Juneja, and A. K. Suri, "Scaling properties of circulation in moderate-Reynolds-number turbulent wakes," *Phys. Rev. Lett.*, vol. 75, pp. 433–436, 1995.
[6] N. Cao, S. Chen, and K. R. Sreenivasan, "Properties of velocity circulation in three-dimensional turbulence," *Phys. Rev. Lett.*, vol. 76, pp. 616–619, 1996.
[7] P. K. Yeung, X. M. Zhai, and K. R. Sreenivasan, "Extreme events in computational turbulence," *Proc. Nat. Acad. Sci. USA*, vol. 112, pp. 12633–12638, 2015.
[8] K. P. Iyer, K. R. Sreenivasan, and P. K. Yeung, "Circulation in high Reynolds number isotropic turbulence is a bifractal," in revision, *Phys. Rev. X*, 2019.
[9] A. N. Kolmogorov, "The local structure of turbulence in an incompressible fluid with very large Reynolds numbers," *Dokl. Akad. Nauk SSSR*, vol. 30, pp. 301–305, 1941.
[10] J. C. R. Hunt, O. M. Phillips, and D. Williams, Eds., *Turbulence and Stochastic Processes: Kolmogorov's Ideas 50 Years On*. Cambridge, UK: Cambridge Univ. Press, 1991.
[11] K. R. Sreenivasan, "Fractals and multifractals in fluid turbulence," *Ann. Rev. Fluid Mech.*, vol. 23, pp. 539–600, 1991.

Zhang, Yang

[1] G. Azimi, R. Dhiman, H.–M. Kwon, A. T. Paxson, and K. K. Varanasi, "Hydrophobicity of rare-earth oxide ceramics," *Nat. Mater.*, vol. 12, 2013.